

H-Mode Behavior Induced by Cross-Field Currents in a Tokamak

R. J. Taylor, M. L. Brown, B. D. Fried, H. Grote,^(a) J. R. Liberati, G. J. Morales, and P. Pribyl
Institute for Plasma and Fusion Research, University of California, Los Angeles, California 90024

D. Darrow and M. Ono

Princeton Plasma Physics Laboratory, Princeton University, Princeton, New Jersey 08543

(Received 26 June 1989)

A sharp transport barrier, accompanied by a bifurcated poloidal rotation and a radial electric field, is formed at the plasma edge by driving a radial current across the outer magnetic surfaces of a tokamak. A decrease in particle transport is observed for negative radial E fields. When the radial current is turned off, the E field and the rotation damp on a time scale comparable with the ion-ion collision time.

PACS numbers: 52.25.Fi, 52.55.Pi, 52.70.Ds

An intensive effort is in progress, worldwide, to correlate the large and growing data base of experimental observations on plasma transport in magnetic fusion containment devices with theoretical models. In particular, the so-called "*H*-mode" regimes in tokamaks have attracted strong interest due to their enhanced particle and energy confinement properties.¹⁻³ The transition of a plasma into the *H* mode is marked by a sudden decrease in the hydrogenic light emission from the plasma edge, followed by a prolonged increase in the plasma density. The reduction of hydrogen light (H_α or H_β) indicates that the incoming neutral particle flux is reduced, presumably because of a decrease of the outgoing plasma flux, leading to a reduction in "recycling." The improvement in the energy confinement is generally less than the increase in particle confinement. *H*-mode measurements also reveal the formation of sharp density and temperature gradients inside the last closed magnetic surfaces, which represents a transport barrier. Despite the magnitude of the effort aimed at modeling the *H* mode, no clear mechanism has been identified, although radial electric fields are thought to play a role.^{4,5} In this Letter, experimental observations confirming the importance of the radial E field and the associated plasma rotation for *H*-mode confinement are presented.

In 1979, electron injection was used to modify the edge potentials in order to reduce ion sputtering in the Macrotron tokamak.⁶ Subsequently, improved particle confinement and a concomitant impurity accumulation were observed,⁷ apparently giving rise to an *H* mode. These effects were attributed to the creation of edge radial electric fields and associated negative plasma potentials much larger in magnitude than $T_e(a)$, where a is the plasma radius. Recently we have extended this earlier work using the new, titanium-gettered, Continuous Current Tokamak (CCT) at the University of California, Los Angeles. The recent experiments clearly show the *H*-mode signatures found in other tokamaks in various limiter, divertor, and auxiliary-heating configurations. The previously seen impurity limitations⁷ have also been eased by new electrode designs.⁸

For the *H*-mode-regime studies, CCT was operated in the pulsed neo-Alcator regime, with central parameters $R=1.5$ m, $a=0.4$ m, $B_t=3$ kG, $I_p=50$ kA, $n_e=5 \times 10^{12}/\text{cm}^3$, $V_{\text{loop}} < 1.5$ V, $T_e > 150$ eV, and $T_i > 100$

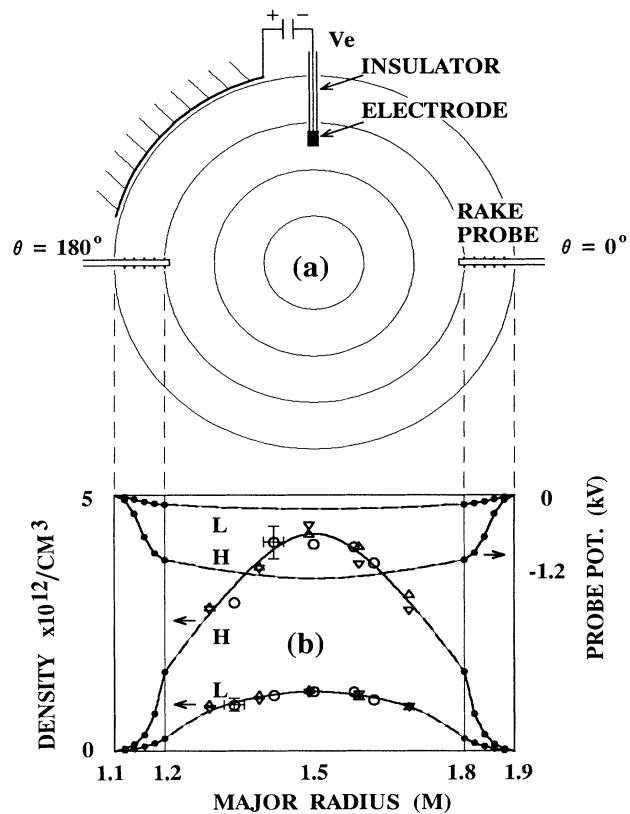


FIG. 1. (a) Cross section of tokamak, $a=40$ cm, showing the location of the exciting electrode, $r_e=25$ cm, and the "rake" probe arrays used for measuring floating potential and edge plasma density in the E -field layer. (b) Edge profiles of potential and density in *L* and *H* modes. The core density values are derived from Abel-inverted microwave interferometer data. Dashed lines represent best estimates of unmeasured floating potentials in the interior.

eV. In this regime the plasma power densities are sufficiently low to permit detailed measurements by Langmuir probes. Our results are thus complementary to the work on the Texas Experimental Tokamak, where the emphasis is on determining the role of density and potential fluctuations on transport⁹ (although the effect of radial fields on fluctuations has been considered^{3,10}).

The radial electric fields are excited by cross-field currents from electrodes located well in the interior of the plasma. This gives rise to *radial current* in the region *interior* to the last closed magnetic surface. Figure 1(a) shows the electrical circuit that allows us to bias the plasma dc potential to negative (or positive) values larger than $10T_e$. We have found that, for the negative bias, both electron-emissive injectors (W, LaB₆) and cold-ion collectors (graphite) produce similar results, provided that the collection surface is large enough to draw sufficient current (typically of order 20 A) and small enough not to form a limiter. As indicated by the potential profile sketched in Fig. 1(b), the potential in the plasma is close to the electrode potential, V_e , for r smaller than the location r_e of the electrode and remains at that value out to a radius $r_b > r_e$, where it has a rapid rise to a slightly positive value in the plasma halo, finally dropping to 0 at the first wall. The region of rapid potential rise, the *E*-field layer as we shall call it, reveals an $\mathbf{E} \times \mathbf{B}$ (6×10^6 cm/sec) rotation of the plasma, which is comparable to the ion thermal speed. The speed of the rotation is directly determined from directional-energy-analyzer data, where we find that $v_\theta = 6 \times 10^6$ cm/sec and $v_\phi < 1 \times 10^6$ cm/sec. Consequently, the fluid velocity along the field lines is negligibly small. The rotation is possible because the applied radial current overcomes the neoclassical damping¹¹ through the θ component of the $\mathbf{J} \times \mathbf{B}$ force.

Most of the data were taken simultaneously, with a number of radial "rake" probe arrays. The location of these arrays in the poloidal plane is shown in Fig. 1(a). For the core region, Abel-inverted values of density taken from microwave interferometer data are shown in Fig. 1(b).

Figure 2 shows the time evolution of the discharge. A cylindrical electrode, of radius 2 cm and height 4 cm, was biased to $V_e = -1.5$ kV at $t = 45$ msec. The floating potential, as measured with a Langmuir probe (crosschecked by the swept I - V characteristics of the probe, giving $V_{\text{float}} = V_{\text{plasma}} - 3T_e$), drops slightly [Fig. 2(d)] and then, as the current slowly rises to a critical value, makes an abrupt transition (within 30 μ sec) to near V_e . The injection current tends to decrease in magnitude at the spontaneous transition [Fig. 2(c)], while the electric field and the plasma rotation increase there. This phenomenon represents a bifurcation in plasma rotation (i.e., two values of rotation are possible for the same current). The sharp transition in the applied current and the measured probe voltages is followed by a

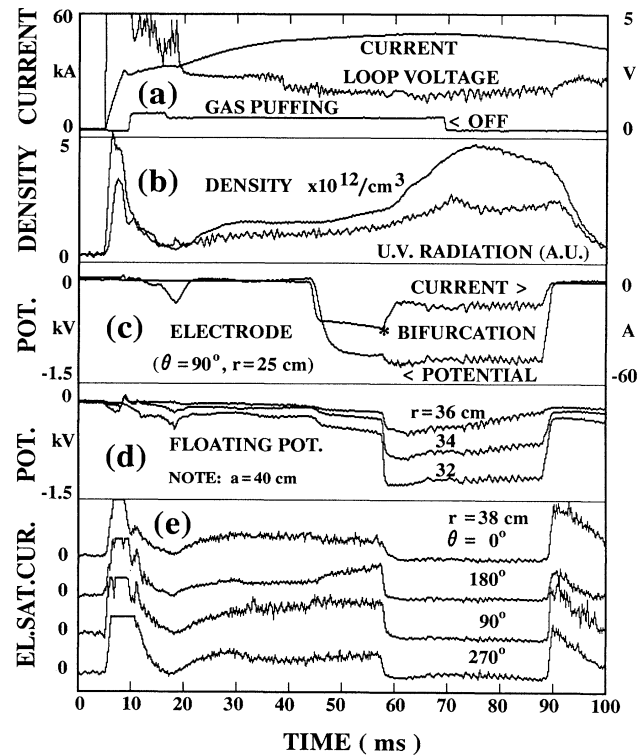


FIG. 2. Time history of tokamak plasma parameters. *H*-mode transition, exhibiting bifurcation, occurs at 58 msec on the graphs. (a) Plasma current, loop voltage, and external gas puffing. (b) uv radiation (not divided by density), showing no accumulation of impurities, and the line-average plasma density. The density increases rapidly after the *H*-mode transition until the gas puffing is turned off (at 70 msec). (c) Electrode current, showing a marked reduction at the transition, and electrode bias, which increases slightly. These results imply a reduction of the radial conductivity at the transition. (d) Data from three of the probes in a rake array indicating an *E* field of 200 V/cm. (e) Electron saturation currents from Langmuir probes placed 2 cm in from the limiter-liner at four poloidal locations. All show the plasma edge density nearly vanishes in this region.

significant increase in particle confinement, as evidenced by the chord-averaged density increase [Fig. 2(b)] and the reduction in recycling (drop in H_β light, not shown in Fig. 2). Some density improvement, however, is present even before the transition, in Fig. 2(b). These effects are also accompanied by a significant but modest ($1.5 \times$) improvement in the coefficient of the density-dependent global neo-Alcator energy confinement time, as determined from parallel-conductivity (giving T_e) and fast-neutral-flux analyses (yielding T_i).

During the application of the electrode bias, the edge puffing rate was not altered until the density had approximately doubled. Then the gas puffing was terminated [Fig. 2(b)], resulting in a slowly decaying density, $\tau > 30$

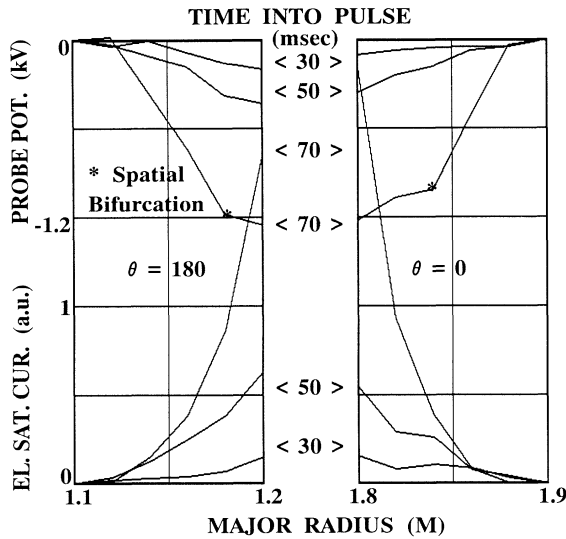


FIG. 3. Radial profiles of the edge region up to 10 cm inside the limiter-liner at various times into the discharge. Transition occurs between the 50- and the 70-msec profiles. The spatial bifurcation point is at the maximum shear. (See Fig. 2.)

msec, perhaps limited by recombination at the electrode and probes. When the potential well is terminated, a rapid decrease of the plasma density is observed ($\tau < 5$ msec), resulting in a large flux to the wall-limiter. This density decay rate is what we observe during normal Ohmic-heating operation of CCT. The direct observation of the particle confinement time is facilitated by the refreshed titanium coating of the plasma-facing components, resulting in low recycling.

Figure 3 shows the profiles of floating potential (the plasma potential is at most 100 V more positive for the innermost probe) and density obtained using the rake probes in the edge region. These profiles represent "snapshots" taken at the times indicated, before and after the transition, which occurs in less than 100 μ sec.

Figure 4 shows a summary of the radial current, floating potential at $r = 30$ cm, and the measured radial conductivity (averaged over the magnetic surface at r , i.e., $\sigma_r = I_r / 4\pi^2 R r E_r$) as a function of applied bias potential. The reduction in recycling light, the loop voltage, the rate of density buildup, and an index (the uv radiation divided by the plasma density) reflecting relative impurity levels are summarized. These data were taken during the biasing phase, with bifurcation only occurring for applied potentials more negative than -150 V; however, transport improvements are present at smaller fields as noted above.

In passing we wish to point out that positive radial E fields and a corresponding reversal in rotation have also been investigated in the plasma edge ($0.8 < r/a < 1.0$) and only deterioration in the transport is seen, including an obvious increase in recycling. For the negative E -field case, correlations with H -mode behavior in other

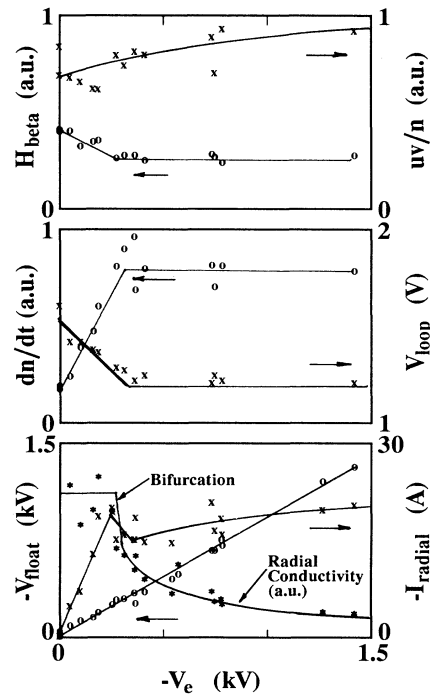


FIG. 4. Variation with electrode bias of H_β intensity, uv radiation normalized to plasma density, time derivative of the density, loop voltage, floating potential at $r = 30$ cm, radial current (injected from the electrode), and the radial conductivity. Particularly notice the reduction of radial conductivity for driving fields larger than that needed for bifurcation. (The transition is masked in this multishot graph due to parameter variations.)

tokamaks include (1) the reduction of recycling as seen in the hydrogen influx light; (2) the increase of the plasma density after the transition, for the same or reduced influx of neutrals; and (3) a rapid (100 μ sec) L -mode- H -mode-like transition to an improved-confinement regime, the speed of which is the consequence of bifurcation.

These results are consistent with the assumption that the poloidal rotation is damped approximately on the ion-ion collision time as advocated in Ref. 12. Since directional-probe measurements show that $v_{||} = 0$, the toroidal rotation, $v_\phi = B_\theta v_\theta / B_\phi$, is small compared to v_θ . Furthermore, in the bifurcated state, the diamagnetic drift is also small compared to v_θ ($\kappa_p / \kappa_r \ll neE_r$). Thus, the poloidal velocity is approximated by E_r / B_ϕ and the poloidal damping is balanced by the θ component of the $\mathbf{J} \times \mathbf{B}$ force, i.e.,

$$J_r B_\phi = nm v_\theta / \tau_p = nm (E_r / B_\phi) v_{ii}, \quad (1)$$

where m is the ion mass and τ_p is taken to be the reciprocal of v_{ii} , the ion-ion collision rate. When the ratio of rotational speed to ion thermal speed exceeds B_θ / B_ϕ , this formula gives a close agreement between calculated

and observed radial current for the edge parameters in CCT ($I_r=20$ A, $R=1.5$ m, $r=35$ cm, $T_i=30$ eV, $B_t=0.3$ T, $n=10^{12}/\text{cm}^3$, $E_r=200$ V/cm). Our analysis does not take into account either the turbulence or the changes in banana orbits as the E field increases. The comparison of the radial current to neoclassical predictions, at small E fields (20 V/cm), where the influence of the poloidal field is relevant, also appears reasonable.

A comprehensive neoclassical description of the poloidal damping force for a wide range of rotational velocities has been obtained by Shaing and Crome¹³ recently. Their results explicitly show that radial currents can lead to bifurcation in the poloidal rotation due to an initial increase in the viscous damping, followed by a decrease as the plasma rotated at higher poloidal speeds.

In conclusion, H -mode-like enhancements of particle confinement ($>10\times$) and modest improvements in the energy confinement ($1.5\times$), both relative to gas puffing to the same density, have been produced in CCT by externally imposed radial currents. The resulting poloidal rotation velocity is close to the ion thermal speed. This large rotation is accompanied by a reduction of the edge-plasma radial electrical conductivity which leads to bifurcation in the radial E field in space and time. In addition, our results suggest that (1) the rapid start of an H mode is associated with poloidal rotation (without an associated rotation parallel to B) and can occur on the time scale of ion-ion collisions; (2) the plasma rotation is driven by radial currents and not E fields; and (3)

the rotation-induced negative E fields are responsible for the improved ion transport.

The authors wish to acknowledge useful discussions with J. M. Dawson and R. R. Weynants. This work was supported by the U.S. Department of Energy under Contracts No. DE-FG03-86ER53225 and No. DE-AC02-76-CH0-3037.

^(a)Permanent address: Central Institute for Electron Physics, Berlin, German Democratic Republic.

¹F. Wagner *et al.*, Phys. Rev. Lett. **49** 1408 (1982).

²K. McGuire *et al.*, in *Proceedings of the Tenth International Conference on Plasma Physics and Controlled Nuclear Research, London, 1984* (International Atomic Energy Agency, Vienna, 1985), Vol. 1, p. 117.

³M. Nagami *et al.*, Nucl. Fusion **24**, 183 (1984).

⁴P. E. Phillips *et al.*, J. Nucl. Mater. **145-147**, 807 (1987).

⁵K. C. Shaing, W. A. Houlberg, and E. C. Crome, Jr., Comments Plasma Phys. Controlled Fusion **12**, 69 (1988).

⁶R. J. Taylor and L. Oren, Phys. Rev. Lett. **42**, 446 (1979).

⁷L. Oren *et al.*, J. Nucl. Mater. **111-112**, 34 (1982).

⁸M. Ono *et al.*, Phys. Rev. Lett. **59**, 2165 (1987); D. S. Darrow *et al.*, Bull. Am. Phys. Soc. **33**, 1933 (1988).

⁹Ch.P. Ritz *et al.*, Phys. Rev. Lett. **62**, 1844 (1989).

¹⁰T. Chiueh, P. W. Terry, P. H. Diamond, and J. E. Seldak, Phys. Fluids **29**, 231 (1985).

¹¹S. P. Hirshman, Nucl. Fusion **18**, 917 (1978).

¹²T. H. Stix, Phys. Fluids **16**, 1260 (1973).

¹³K. C. Shaing and E. C. Crome, Jr., this issue, Phys. Rev. Lett. **63**, 2369 (1989).